JOURNAL OF AGRICULTURAL AND FOOD CHEMISTRY

Article

pubs.acs.org/JAFC

Quantum Dots Capped with Dummy Molecularly Imprinted Film as Luminescent Sensor for the Determination of Tetrabromobisphenol A in Water and Soils

Yi-Ping Chen, Da-Ning Wang, Yu-Min Yin, Li-Yun Wang, Xiang-Feng Wang, and Meng-Xia Xie*

Analytical & Testing Center of Beijing Normal University, Beijing 100875, China

ABSTRACT: Molecularly imprinted film with diphenolic acid (DPA) as dummy template molecule has been grafted on the surface of Mn-doped ZnS quantum dots (QDs) to develop a selective and sensitive sensor for rapid determination of tetrabromobisphenol A (TBBPA) in water and soils. The obtained DPA-MIP-QDs sensor has distinguished selectivity and high binding affinity to TBBPA. The fluorescence quenching fractions of the sensor presented a satisfactory linearity with the concentrations of TBBPA in the range of 0.1−100 μM, and its limit of detection can reach 0.015 μM. The sensor has been successfully applied to determine the TBBPA in water and soil samples, and the average recoveries of the TBBPA at various spiking levels ranged from 80.2% to 96.5% with relative standard deviation below 8.0%. The results provided a clue to develop sensors for rapid determination of hazardous materials from complex matrixes.

KEYWORDS: *quantum dots, tetrabromobisphenol A, dummy molecularly imprinted film, sensor, soils*

INTRODUCTION

The importance of (bio)chemical sensors in analytical science has been greatly accepted, and the development of the portable analytical devices can simplify and miniaturize the whole analytical process due to their ease of use, good selectivity, high sensitivity, and short analysis time.[1−5] However, the design of (bio)chemical sensors suffers from two main limitations. One is the instability of the biological sensing component, and the second is how to obtain the physicochemical transducers as small as possible.[6] To solve these problems, increasing attention has been paid to the nanomaterials and nanotechnologies to develop new materials for biological recognition and signal transduction elements.[7,8]

Over the past decade, quantum dots (QDs) have largely contributed to the development of (bio)chemical sensors due to their excellent optical properties over the traditional fluorescent dyes,[9−11] and the surface of QDs can be functionalized or modified to obtain various probes for chemical and biochemical optical sensing.[12−14] The Mn-doped ZnS QDs have drawn increasing attention in recent years due to its low toxicity.[15,16]

Molecular imprinting technique can obtain materials with numerous distinct advantages, such as inherently chemical, mechanical, and thermal stability, and high selectivity to template molecules.[17,18] As compared to biomacromolecular receptors, molecularly imprinted polymers (MIPs) possessed a simple process for preparation, economic availability, and high stability.[19] Consequently, MIPs have been widely considered for the mimics of natural molecular receptors, affinity, or catalytic sensors, and were successfully applied to the development of electrochemical, piezoelectric, and surface plasmon resonance sensors.[20−22] Nevertheless, the conventional MIPs have some inconveniences because their preparation processes were bulk or precipitation polymerization, and so the residues of template molecules and the recognition sites were embedded deeply in the matrix, which probably resulted in the leakage of the template and poor site accessibility. Surface molecular imprinting polymers[23−25] with dummy templates strategy can overcome these drawbacks of the traditional MIPs, and the obtained sorbents have adequate selectivity, more accessible binding sites, fast mass transfer rate, and binding kinetics. Some polar groups, such as carboxyl or amino, can be introduced to the dummy template molecules to increase the interaction of template and functional monomers, which is the key factor to the affinity of the MIPs.[26,27]

Combining the high selectivity of MIPs and excellent optical properties of QDs would develop sensitive and specific sensors for recognizing an analyte. The MIPs on the surface of the sensor can specially bind the target analyte, which bring about the fluorescence quenching of the sensor,[28] and the degree of quenching may be related to the amount of the target analyte.[29] There have been several applications based on surface molecular imprinting QDs sensors for the determination of TNT,[30] pentachlorophenol,[28] and 4-nitrophenol,[29] and one-pot urinalysis was also achieved by molecularly imprinted poly(ethylene-*co*-vinylalcohol)/quantum dot composite nanoparticles.[31] However, there would be potential venture of leakage for the template molecules, and sometimes the cavity of the high binding affinity to the analytes on the MIP film may not be achieved when the analytes were selected as template molecules, which would impair the selectivity and sensitivity of the sensors.

Tetrabromobisphenol A (TBBPA) is usually utilized in epoxy resins, polycarbonate, and phenolic resins as reactive flame retardant, and is also used with diantimony trioxide in engineering plastics as additive type flame retardant.[32] In certain conditions, TBBPA can be transformed into bisphenol

Received: June 22, 2012
Revised: October 9, 2012
Accepted: October 9, 2012
Published: October 9, 2012

dx.doi.org/10.1021/jf3026138 | *J. Agric. Food Chem.* 2012, 60, 10472−10479

A (BPA) or TBBPA dimethyl ether (TBBPA DME), which has estrogenic activity and significantly thyroid hormonal activities;[33,34] therefore, the determination approaches for TBBPA in various matrixes have drawn much attention in recent years. Chromatographic methods and related techniques have been frequently applied to the identification and quantification of TBBPA and related compounds.[35−39] Although these methods are sensitive and reliable, they are time-consuming, and so it is very essential to develop a rapid, sensitive, simple, and low-cost method to monitor the trace TBBPA in the environmental samples.

The purpose of this subject was to develop a high affinity DPA-MIPs-QDs sensor for selective determination of trace TBBPA in water and soil samples. DPA was chosen as dummy template, and the MIP film was capped on the surface of Mn-ZnS QDs via a sol−gel process. The thickness of the MIP film and the influence of pH on the optical properties of the sensors were investigated, and the selectivity and response time of the sensor were characterized. The obtained DPA-MIPs-QDs sensor can selectively and sensitively detect trace TBBPA in complicated environmental samples using high-throughput mode especially when combined with DPA-MIP affinity solid-phase extraction (SPE) procedures. Moreover, this sensor has economic advantage over chromatographic methods.

MATERIALS AND METHODS

Materials and Reagents. DPA, TBBPA, bisphenol A (BPA), diethylstilboestrol (DES), nonylphenol (NP), and trichlorophenol (TCP) were purchased from Acros Organics (NJ). Silica gel particles, 75−150 μm (100−200 mesh), $ZnSO_4{\cdot}7H_2O$, $MnCl_2{\cdot}4H_2O$, and $Na_2S{\cdot}9H_2O$ were provided by Sinopharm Chemical Reagent Beijing Co., Ltd. (Beijing, China). 3-Aminopropyltriethoxysilane (APTES), tetramethoxysilane (TEOS), and 3-mercaptopropyltriethoxysilane (MPTS) were obtained from J&K Chemical. Ltd. (Beijing, China). Ultrapure water (18.3 MΩ) obtained from Millipore Milli-Q purification system (Boston, America) was used to prepare solutions. $NaHCO_3$−Na_2CO_3 buffer solution (0.1 mol L^{-1}) was involved in the experiment, and the pH of this buffer was adjusted by the volume ratio of $NaHCO_3/Na_2CO_3$. All reagents were analytical grade and used without further purification.

Synthesis of Sensors. The Mn-doped ZnS QDs were prepared according to the reported methods with some modification.[28] In a 250 mL three-necked flask, 8.97 g of $ZnSO_4$, 0.493 g of $MnCl_2$, and 100 mL of water were sequentially added, and the solution was stirred under argon gas at room temperature for 15 min. Next, 25 mL of aqueous solution containing 7.5 g of Na_2S was added dropwise, and the mixture was kept stirring for 30 min. Thereafter, 25 mL of ethanol solution and 391.5 μL of MPTS were added, and the solution was kept stirring for 20 h. The product was centrifuged and washed with ethanol (30 mL) two times, and then dried in a vacuum (42 °C) to obtain MPTS-capped Mn-doped ZnS QDs.

To a 50 mL flask were added 65.4 mg of DPA (template) in 10 mL of methanol solution and 200 μL of APTES (functional monomer), and the solution was stirred for 30 min, and then 800 μL of TEOS (cross-linking monomer) was added, and the solution was kept stirring for 5 min. Thereafter, 500 mg of MPTS-capped Mn doped ZnS QDs and 0.5 mL of 6% $NH_3{\cdot}H_2O$ (catalyst) were added, and the reaction was carried out for 16 h under stirring. The products were centrifuged and washed with 50 mL of ethanol to remove the unreacted monomers, and then dried in a vacuum at 42 °C for 12 h. To remove the template, the MIP-capped Mn-doped ZnS QDs was washed with methanol (60 mL) four times (the elution was monitored by HPLC until no template can be detected), and then it was dried under vacuum at 42 °C for 12 h.

The nonimprinted polymer (NIP) capped Mn-doped ZnS QDs were synthesized in the same process without addition of the dummy template.

Characterization. Infrared spectra of the QDs, DPA-MIP-QDs, and NIP-QDs sensors were collected by a Nicolet Nexus 670 FT-IR spectrometer (Thermofisher, Madison, WI) with a diffuse reflectance accessory. The samples were mixed with KBr powder, and then scanned in the range of 4000−650 cm^{-1} with 256 scans at the resolution of 4 cm^{-1}. The morphology and microstructure of sensors were characterized by a field emission scanning electron microscope (SEM) (Hitachi, Japan).

Fluorescence Measurements. The fluorescence measurements were performed on an F-4500 spectrofluorometer (Hitachi, Japan) with the excitation wavelength of 350 nm when the spectrofluorometer was set in the fluorescence mode; the slit widths of excitation and emission were 10 and 20 nm, respectively. The photomultiplier tube (PMT) voltage was 950 V.

In a 10 mL test tube, 1.0 mL of MIP- or NIP-QDs suspension (0.1 mg mL^{-1}) with 0.1 mol L^{-1} Na_2CO_3−$NaHCO_3$ buffer, and a given concentration of analyte standard solution or Na_2CO_3−$NaHCO_3$ (0.1 mol L^{-1}, pH = 9.16) buffer, were sequentially added. The mixture was then diluted to volume with buffer solution and ultrasonicated for 10 min before measurement.

A fluorescence microplate reader (Thermo scientific) with an excitation/emission at 300/582 nm was utilized to attain high-throughput fluorescence signal using 96-well plates, and its excitation bandwidth was 5 nm with a step size of 2 nm. Calculations were performed with OriginPro7.5 software.

Specificity. BPA, DES, NP, and TCP were involved to evaluate the specificity of MIP-QDs sensor. The selective assays were investigated by using the same concentration of TBBPA, BPA, DES, NP, and TCP on MIPs-QDs and NIP-QDs sensors, respectively. The measuring procedures were as described above.

Time Response and Dose Effect of MIP-QDs Sensor to TBBPA. The MIP-QDs or NIP-QDs sensor was exposed to 20 μM of TBBPA, respectively. The degree of fluorescence quenching was monitored at certain time intervals (1, 4, 7, 10, 12, and 15 min).

Different concentrations of TBBPA (0, 0.05, 0.1, 0.2, 1, 5, 10, 20, 40, 60, 80, and 100 μM) were added into 0.1 mg mL^{-1} MIP-QDs or NIP-QDs suspension, respectively, and then their fluorescence spectra were collected.

Pretreatment of Samples. DPA-imprinted polymers were prepared with a sol−gel process at the surface of the silica gel particles according to our previous report with some modification.[27] In brief, DPA (1.830 g) was dissolved in 10.0 mL of methanol/chloroform (1:3, v/v) solution, and then mixed with 4.0 mL of APTES. After being stirred for 30 min, 10.0 mL of TEOS was added, and the mixtures were stirred for another 5 min. 4.0 g of activated silica gel, which was dispersed in 10.0 mL of methanol:chloroform (1:3, v/v) solution, and 2.0 mL of 1.0 mol L^{-1} HAc (catalyst) were subsequently added to the above mixtures, and the solution was incubated for 15 h at room temperature under stirring. The products were isolated by centrifugation at 5000 rpm for 10 min and then dried under vacuum at 70 °C for 12 h. To remove the template DPA, the polymers were washed with a mixture of methanol (50 mL) and 1.0 mol L^{-1} HCl (50 mL) four times, and then with NaOH (0.50 mol L^{-1}) and pure water until the pH of the solution reached neutral. The MIP sorbent was dried under vacuum at 70 °C for 12 h.

SPE Procedures. 500 mg of DPA-MIPs sorbent was packed in empty polypropylene SPE cartridges. The sorbent was activated with 5.0 mL of methanol, and then 20 mL of sample solution was loaded on the SPE cartridge with a flow rate of 1 mL min^{-1}. The analyte was eluted with a 1 mL solution of methanol:acetic acid:ultra pure water (90:5:5, v/v), and the eluent was dried under a stream of nitrogen gas at 45 °C. Finally, the residues were dissolved in 1 mL of methanol/$NaHCO_3$−Na_2CO_3 buffer solution (1:9, v/v) for sensor determination.

Water samples were collected from local river and lake in Beijing, and the samples were centrifugated and the supernatants mixed with methanol at the volume ratio of 1:1, and 20 mL of the solution was loaded on the SPE cartridges as per the procedures described above.

Surface soil and sludge samples were collected from the E-waste plant in Zhe Jiang province (China). The samples were air-dried and

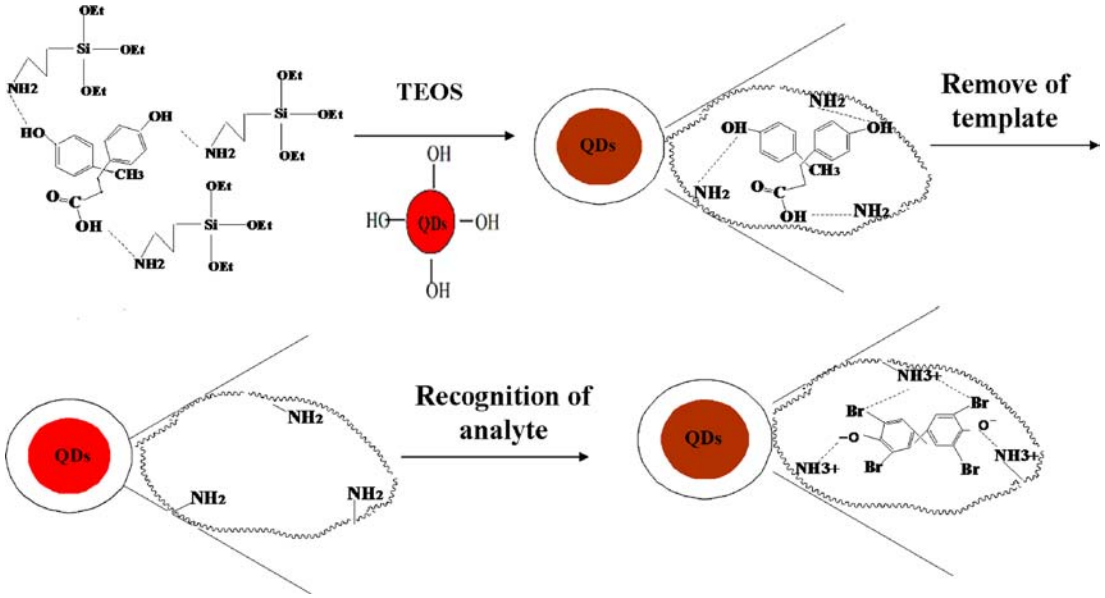

Figure 1. Schematic procedures for the preparation of DPA-MIP-QDs sensor.

sieved (2 mm). 1.0 g of homogeneous sample was vortex-mixed with 20 mL of methanol and dichlormethane (2:8, v/v) solution for 15 min, and then ultrasonicated for another 15 min. The extract was centrifugated for 2 min at the speed of 4000*g*, and the supernatant was loaded on the SPE column as the procedures described above. If the samples were verified to be free of TBBPA, the spiking recoveries were performed with different concentration levels (0.05, 0.5, and 5 μM for water samples and 1, 2, and 10 μM for soil and sludge) of TBBPA via the same procedures, and each sample was assayed six times (n = 6).

RESULTS AND DISCUSSION

Preparation of DPA-MIP-QDs Sensor. Figure 1 shows the schematic procedure for the preparation of DPA-MIP-QDs sensors. DPA was used as dummy template molecule to form MIP film on the surface of QDs. The carboxyl and phenolic hydroxyl groups of DPA can form strong hydrogen bonding with the amino groups of the functional monomer (APTES) in the preorganization process (see Figure 1), which would allow the formation of appropriately sized recognition cavities for the intended target molecule,[40] and thus provide the basis of the development of a sensor. The MIP film on the surface of the QDs, as a recognition element, can especially rebind trace TBBPA in complicated matrix, which will bring about fluoresce quenching due to the interaction between QDs and TBBPA, and the degree of quenching would be related to the amount of target analyte.[41]

The thickness of the MIP film was a key factor that affects the site accessibility and mass-transfer resistance of an analyte.[40] The effects of the thickness for the MIP film on the binding affinity of the QDs sensors were evaluated. The binding affinities (K_A) of TBBPA on the QDs sensors can be obtained from the slopes of the double reciprocal curves based on the following equation:[42]

$$\frac{F_0}{F_0 - F} = 1 + K_A^{-1}[Q]^{-1}$$

F_0 and F are the fluorescent intensities of the sensors in the absence and presence of TBBPA, respectively, and $[Q]$ is the molar concentration of TBBPA.

The relative K_A of the MIP-QDs sensors to that of NIP-sensors represented the selectivity of the MIP films, which can be defined as the imprinting factor (IF).[30] The thickness of the MIP films was regulated by altering the ratios between the total amount of reactants for preparing the MIP films and that of QDs sensor, and the influences of the ratios on the binding affinities (K_A) of the sensors were listed in Table 1.

Table 1. Effect of the Thickness for the MIP Film on the Binding Affinity and Selectivity of the Sensors

ratio of MIP/QDs	$K_{A,MIP}$	$K_{A,NIP}$	IF = $K_{A,MIP}/K_{A,NIP}$
4:1	8003 ± 321	4201 ± 348	1.90
4:2	10 180 ± 313	4031 ± 316	2.52
4:3	12 376 ± 487	4448 ± 424	2.78
1:1	6967 ± 239	5371 ± 259	1.30

It can be seen from the data in Table 1 that the K_A of the NIP-QDs sensor has minor variations with reducing the thickness of film (ratio of MIP to QDs from 4:1 to 4:3), while that of MIP-QDs sensor significantly increased, which illustrated that the decrease of the thickness for the MIP film was favorable to raise the quenching efficiency and binding affinity of the QDs sensor to TBBPA. However, the K_A of MIPs-QDs sensor was obviously decreased when the ratio of MIP to QDs reached to 1:1, and it indicated that the selectivity and sensitivity of the QDs sensor were reduced. Generally, the binding capacity of the MIP would be low if the thickness of the film was too thin,[28] and so suitable MIP film could be obtained when the ratios of MIP to QDs were 4:3 or 4:2. The stabilities of the MIP-QDs sensors were investigated, and it has been found that the sensor obtained in the ratio of 4:2 (MIP to QDs) was more stable than that in the ratio of 4:3. The fluorescent intensity of sensor for the ratio of 4:2 did not decrease significantly in a month, while that for the ratio of 4:3 reduced nearly by one-half, and so the MIP films on the QDs were prepared with the ratio of 4:2.

It should be mentioned that the post-treatment procedures in the preparation processes of the MIP-QDs sensors have obvious effects on their quenching efficiency. If the sensors

were dried twice at 42 °C for 12 h, before and after removing the template, their K_A was about 9700 M^{-1}, while the K_A was about 7300 M^{-1} when the sensors were only dried after removing the template. The results revealed that the imprinted binding cavities of the sensors probably need retrogradation at a suitable temperature before removal of the template, and, in this case, the binding site would become more stable.

Characterization of the Sensors. Figure 2 shows the FT-IR spectra of the sensors before and after capping the films on

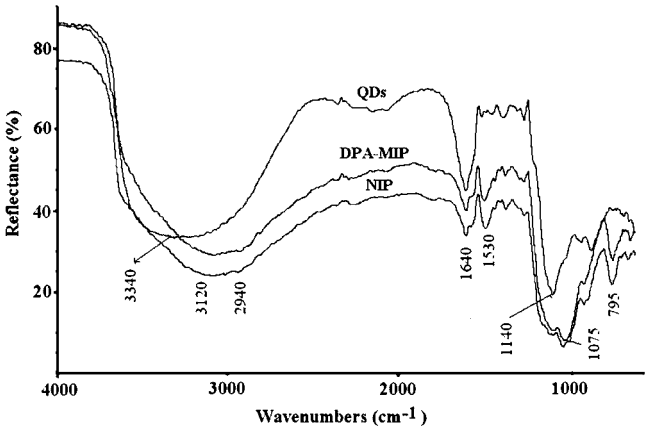

Figure 2. FT-IR diffuse reflectance spectra of QDs; DPA-MIP-capped Mn-doped ZnS QDs (DPA-MIP); and NIP-capped Mn-doped ZnS QDs (NIP).

the surface of QDs. The bands at about 3340, 1640, and 1140 cm^{-1} were the characteristic vibration absorptions of the −OH and Si−O on the surface of the MPTS-capped ZnS QDs. For the MIP- and NIP-QDs sensors, the strong and broad bands at 3120 cm^{-1} and the weak shoulder peak at 2940 cm^{-1} can be ascribed to stretching vibration of N−H and $-CH_2-$, respectively, and the moderate band at 1530 cm^{-1} was attributed to the bending vibrations of N−H, which suggested the existence of the aminopropyl group on the surface of the sensors. The strong band at 1075 cm^{-1} and the moderate peak at 795 cm^{-1} were the asymmetric stretching adsorption of Si−O−Si and vibration of Si−O groups. The results illustrated that APTES and TEOS were successfully grated on the surface of the MPTS-capped ZnS QDs.

The SEM image (see Figure 3a) shows that the diameter of the MPTS-capped ZnS QDs was about 20 nm and that of the MIP-capped QDs was about 100 nm (Figure 3b), which suggested that the MIP films have been coated on the surface of QDs.

Effect of pH. The pH environment had a significant influence on the affinity of MIP film and the stability of QDs

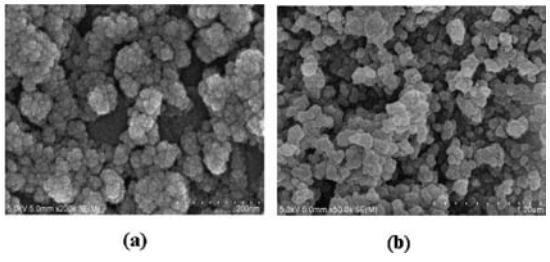

Figure 3. SEM images of Mn-doped ZnS QDs (a) and MIP capped on Mn-doped ZnS QDs (b).

sensors.[43] The binding affinities of the sensors to TBBPA under various pH conditions were evaluated using double reciprocal curves of $F_0/(F_0 - F)$ versus $[Q]^{-1}$. The IF of K_A for the sensors was 2.50, 2.79, 2.02, and 2.08 when the pH were 8.0, 9.16, 10.14, and 10.53, respectively, and the results indicated that the MIP-QDs sensors have relative high binding affinities to TBBPA at pH 9.16. The pK_a of TBBPA was 7.5 (pK_{a1}) and 8.5 (pK_{a2}), and the two phenolic hydroxyl groups of TBBPA would be more effectively deprotonated at pH 9.16 and existed in anion forms. It illustrated that the binding force of TBBPA to the MIP-QDs sensors was mainly ionic interaction between the anion of TBBPA and the $(CH_2)_3NH_3^+$ cation in the binding cavity. At higher pH conditions, the binding affinities tended to decrease possibly because of the participation of the $-OH^-$ with the interactions, and a high concentration of $-OH^-$ would impair the binding affinity of the sensor to TBBPA. Thus, pH 9.16 was selected in the following experiments.

Specificity of MIP-QDs Sensor to TBBPA. Figure 4 shows the relationships between the fluorescence quenching fractions $(F_0/F)^{-1}$ of the MIP- and NIP-QDs sensors and the concentrations of TBBPA and its analogues, BPA, DES, NP, and DCP, which can evaluate the selectivity of the sensors.

It can be seen from Figure 4a that the fluorescence quenching fractions of the DPA-MIP-QDs sensor induced by TBBPA were significantly higher than those of its analogues at all concentration levels, and the differences of the quenching fractions between the analogues were not obvious. The results showed that the analogues cannot effectively enter into the cavities on the surface of the sensor to cause fluorescence quenching, and it demonstrated that the DPA-MIP-QDs sensor had high selectivity for TBBPA. In contrast, the fluorescence quenching responses of the NIP-QDs sensor induced by TBBPA (see Figure 4b) were inferior as compared to that of the MIP-QDs sensor, and the fluorescence quenching fractions were similar between TBBPA and its analogues. It illustrated that the NIP-QDs sensors have poor selectivity for these compounds and implied that the imprinting cavity left by removal of the dummy template on the DPA-MIP-QDs sensors gave more chances for the analyte to access the receptor sites.

It was interesting to note that the MIP-QDs sensor has no selectivity for BPA, whose structural skeleton was similar to that of TBBPA. The pK_a of BPA is 9.5, and the phenolic hydroxyl group of BPA cannot be dissociated at pH 9.16, and so the ionic interaction of BPA and the binding cavity could not be formed. The absence of −Br in the molecule of BPA may be another factor. The −Br of TBBPA possibly could bind with the $-NH_3^+$ cations in the cavity, which would improve the binding affinity of TBBPA to the sensor.

Time Response and Dose Effect of MIP-QDs Sensor to TBBPA. Figure 5 shows the fluorescence quenching fractions at various time intervals when the MIP- and NIP-QDs sensors were exposed to TBBPA (20 μM), respectively. The fluorescence intensities of the sensors were obviously quenched after addition of TBBPA for 1 min, while the differences of the quenching fractions between the MIP-QDs and NIP-QDs sensors were significant, indicating that the MIP-QDs sensor has higher sensibility for TBBPA than does NIP-QDs sensor. As shown in Figure 5, the fluorescence quenching fractions of the MIP-QDs sensor slowly increased until 10 min, and then the alterations were becoming unobvious with further prolonging of the interaction time, while that for NIP-QDs sensor cannot achieve stabilization until 15 min, which illustrated a lack of specific binding of TBBPA to the NIP

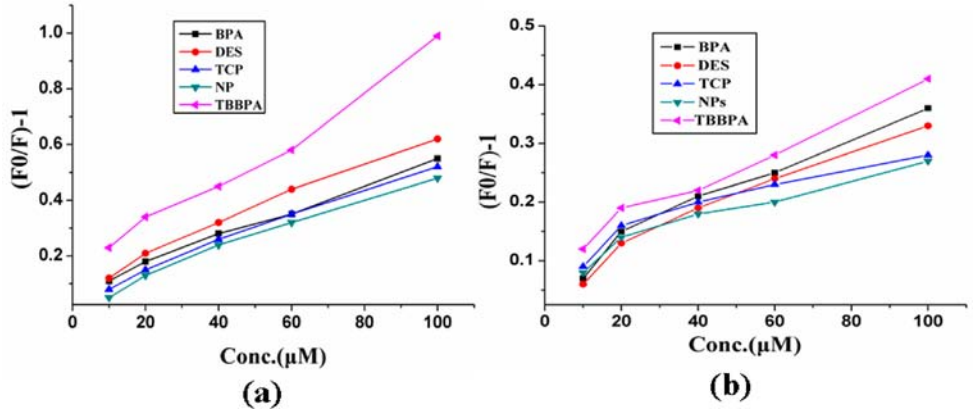

Figure 4. Fluorescence quenching fractions of DPA-MIP-QDs (a) and NIP-QDs (b) sensors versus various concentrations of TBBPA and its analogues BPA, DES, NP, and TCP.

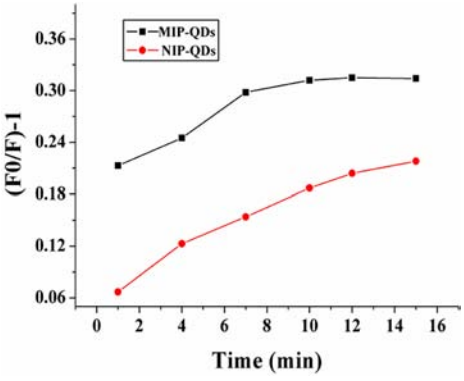

Figure 5. Time response:fluorescence quenching fractions of MIP-QDs (■) and NIP-QDs (red ●) sensors after exposure to TBBPA for 1, 4, 7, 10, 12, and 15 min, respectively.

film of the sensor. The results further demonstrated that the cavities on the MIP film of the MIP-QDs sensor can specifically capture the analytes, and the sensor can be utilized to determine the TBBPA rapidly and steadily, which was especially important for the following high-throughput detection of TBBPA.

The dose effect can provide valuable parameters for the sensitivity and limit of detection (LOD) of the sensor and the relationship for the degree of fluorescence quenching with the concentration of TBBPA. To ascertain these parameters, the fluorescence quenching of the MIP- and NIP-QDs sensors with various concentrations of TBBPA ranging from 0 to 100 μM was measured, respectively, and it has been found that the fluorescence of the sensors gradually quenched with increasing concentrations of TBBPA (see Figure 6a and c). Figure 6b and d shows the curves for the fluorescence quenching fractions of the sensors versus the concentrations of TBBPA. The linear regression curve for DPA-MIP-QDs sensor presented a satisfactory linearity in the concentrations of TBBPA ranging from 0.1 to 100 μM with the regression coefficient of 0.993, which provided the foundation for quantitative determination of TBBPA in samples. The limit of detection (LOD) of the DPA-MIP-QDs sensor can be achieved to be 0.015 μM (8.14 ng/mL), which was determined from 3 times the standard deviations for the fluorescence quenching fractions (n = 6). It can be also noted from Figure 6d that the fluorescence quenching fractions of the NIP-QDs sensor were also linear with the concentrations of TBBPA, while the sensor was relative insensitive and lacked specificity. The LOD of the MIP-QDs sensor for TBBPA was similar to or lower than those of the chromatographic method for the determination of TBBPA,[27] BPA,[25,39] and DES [24] in various matrixes if considering the enrichment factors in the pretreatment procedures. However, the developed sensors can measure the target analyte of samples rapidly and in low cost, which have advantages over the chromatographic approaches.

There was no overlapping between the UV absorption band of TBBPA (at about 290 nm, figure not shown) and the fluorescence emission band of the sensor, which was suited on 590 nm (see Figure 6), and so the fluorescence quenching mechanism of the sensor induced by TBBPA was not fluorescence resonance energy transfer,[44] but probably electron transfer fluorescence quenching.

To improve the efficiency for determining the TBBPA in samples, the suitability of the DPA-MIP QDs sensor for high-throughput detection using microtiter plate reader was investigated. Three concentration levels of TBBPA (0.5, 1, and 5 μM) were determined by the microtiter plate reader and fluorescence spectrophotometer, respectively. The results obtained by the two approaches matched satisfactorily and have no significant differences, and it demonstrated that the MIP-QDs sensors can act as a novel high-throughput approach for determination of TBBPA in samples, which was also important for further developing portable fluorescence detectors to promote the application of MIP-QDs sensors.

Spiking Recoveries of TBBPA in Different Matrixes. The DPA-MIP QDs sensor has been applied for the determination of TBBPA in water samples (tap water, river water, and lake water), soils, and sludges. To promote the sensitivity of the sensor and suitability for complex matrixes, the dummy template (DPA) surface molecularly imprinted polymers (SMIP) on the surfaces of silica gel particles were prepared [27] as sorbents of solid-phase extraction (SPE) for enrichment and purification of TBBPA in samples. After the water samples and the extracts of soils and sludges were pretreated with the SMIP-SPE procedures, the trace TBBPA in samples can be significantly enriched and the matrix interferences were effectively eliminated, thus the sensitivity of the sensor can be significantly increased. The average recoveries and relative standard deviations at various spiking levels for the determination of TBBPA in spiked samples with DPA-MIP QDs sensor coupled to the SMIP-SPE pretreatment procedures were listed in Table 2. The data in Table 2 showed

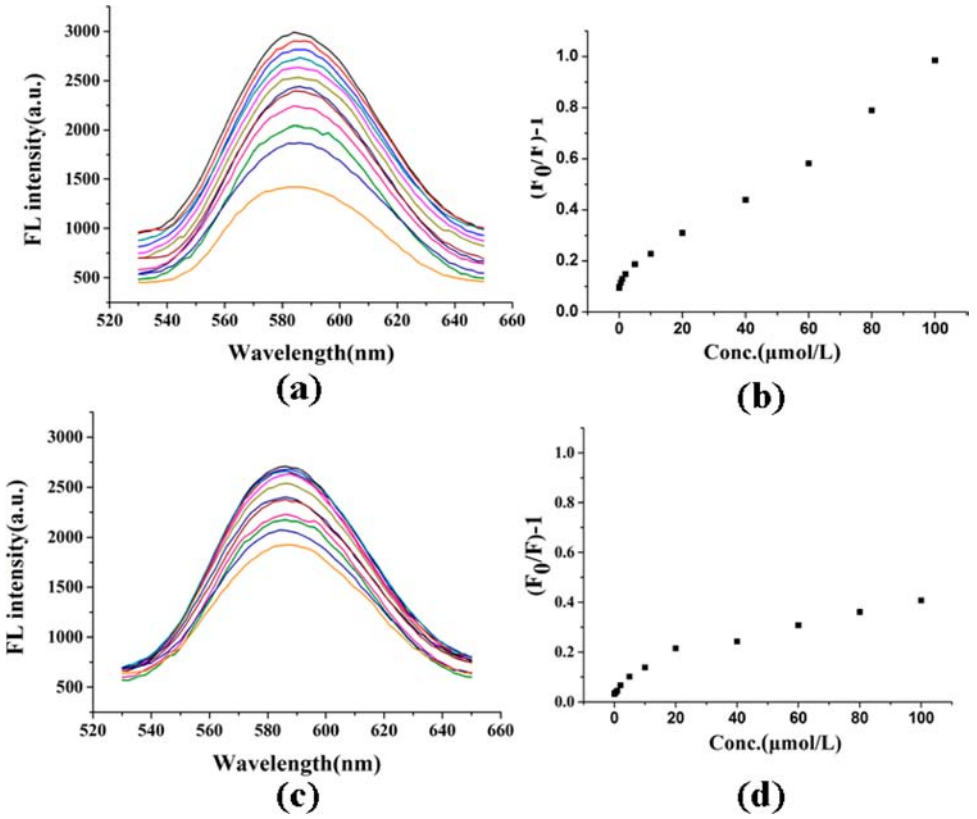

Figure 6. Fluorescence emission spectra of MIP-QDs (a) and NIP-QDs (c) after exposure to various concentrations of TBBPA (0, 0.05, 0.1, 0.2, 1, 5, 10, 20, 40, 60, 80, and 100 μM). Fluorescence quenching fractions of MIPs-QDs (b) and NIP-QDs (d) sensors versus various concentrations of TBBPA.

Table 2. Average Recoveries and Relative Standard Deviations of TBBPA at Various Spiking Levels for Different Matrixes[a]

samples	spiked (μM)	recovery (%)	RSD% (n = 6)
tap water	0.05	92.7	6.3
	0.5	93.4	4.8
	5	96.5	2.9
river water	0.05	92.3	5.2
	0.5	94.2	4.5
	5	98.6	2.2
lake water	0.05	90.3	5.5
	0.5	89.8	2.8
	5	92.2	3.4
soil	1	86.2	7.5
	5	85.6	5.5
	10	87.3	4.4
sludge	1	80.2	7.9
	5	82.7	5.3
	10	83.9	3.8

[a]The enrichment factors for water samples were 10, and for soil and sludge were 1.

that the average recoveries of TBBPA were in the range of 89.8−96.5% with RSDs below 6.3% for water samples, and 80.2−87.3% with RSDs below 8.0% for soils and sludges. The results illustrated that the developed MIP-QDs sensor was suitable to determine TBBPA in samples; especially when coupled with SMIP-SPE pretreatment procedures, the sensitivity of the sensor would be significantly improved and the LOD of the method could be evidently lowered.

A novel molecularly imprinted polymer capped on Mn-doped ZnS QDs sensor has been prepared using diphenolic acid as dummy template molecule. The effects for the thickness of the MIP film on the quenching efficiency and binding affinity of the sensor have been optimized, and it has been found that a stable fluorescence sensor with high binding affinity to TBBPA can be obtained when the ratio for the total amount of reactant to prepare the MIP film with that of QDs was 4:2. At pH 9.16, the DPA-MIP-QDs sensor has high binding affinity to TBBPA, which illustrated that their main binding force was the ionic interaction between the anionic form of TBBPA and the cavity. The −Br of TBBPA can also bind with the $-NH_3^+$ cations in the cavity via ionic binding to improve the selectivity of the sensor. The developed sensor has distinguished selectivity and can specifically recognize TBBPA with rapid response time (10 min). The fluorescence quenching fractions of the sensor presented a satisfactory linearity with the concentrations of TBBPA in the range of 0.1−100 μM, and its limit of detection can reach 0.015 μM. DPA dummy template molecularly imprinted polymers on the surface of silica gel particles were also prepared and used as the sorbents of solid-phase extraction for purification and enrichment of TBBPA in samples. The DPA-MIP QDs sensor combined with the pretreatment procedures has been successfully applied to determine TBBPA in water samples, soils, and sludges. The results demonstrated that the polar groups of the dummy template molecule, especially the carboxyl group, can interact with the monomers via a strong hydrogen bond and form high affinity binding cavities for recognizing the analyte, which is beneficial to further developing sensitive MIP-QDs sensors.

AUTHOR INFORMATION

Corresponding Author

*Tel.: +86-10-58807981. Fax: +86-10-5880007. E-mail: xiemx@bnu.edu.cn, mengxia-xie@263.net.

Notes

The authors declare no competing financial interest.

REFERENCES

(1) Ko, S.; Grant, S. A. A novel FRET-based optical fiber biosensor for rapid detection of Salmonella typhimurium. *Biosens. Bioelectron.* **2006**, *21*, 1283−1290.

(2) Ligler, F. S. Perspective on optical biosensors and integrated sensor systems. *Anal. Chem.* **2009**, *81*, 519−526.

(3) Fan, X. D.; White, I. M.; Shopova, S. I.; Zhu, H. Y.; Suter, J. D.; Sun, Y. Z. Sensitive optical biosensors for unlabeled targets: A review. *Anal. Chim. Acta* **2008**, *620*, 8−26.

(4) John, M. Small molecule immunosensing using surface plasmon resonance. *Sensors* **2010**, *10*, 7323−7346.

(5) Plata, M. R.; Contento, A. M.; Ríos, A. State-of-the-art of (bio) chemical sensor developments in analytical Spanish groups. *Sensors* **2010**, *10*, 2511−2576.

(6) Chafer-Pericas, C.; Maquieira, A.; Puchades, R. Fast screening methods to detect antibiotic residues in food samples. *TrAC, Trends Anal. Chem.* **2010**, *29*, 1038−1049.

(7) Menaker, A.; Syritski, V.; Reut, J.; Opik, A.; Horvath, V.; Gyurcsanyi, R. E. Surface-imprinted conducting polymer microrods for selective protein recognition. *Adv. Mater.* **2009**, *21*, 2271−2275.

(8) He, Y.; Lu, H. T.; Sai, L. M.; Su, Y. Y.; Hu, M.; Fan, C. H.; Huang, W.; Wang, L. H. Microwave synthesis of water-dispersed CdTe/CdS/ZnS core-shell-shell quantum dots with excellent photostability and biocompatibility. *Adv. Mater.* **2008**, *20*, 3416−3421.

(9) Peng, C. F.; Li, Z. K.; Zhu, Y. Y.; Chen, W.; Yuan, Y.; Liu, L. Q.; Li, Q. S.; Xu, D. H.; Qiao, R. R.; Wang, L. B.; Zhu, S. F.; Jin, Z. Y.; Xu, C. L. Simultaneous and sensitive determination of multiplex chemical residues based on multicolor quantum dot probes. *Biosens. Bioelectron.* **2009**, *24*, 3657−3662.

(10) Ruedas-Rama, M. J.; Hall, E. A. Analytical nanosphere sensors using quantum dot enzyme conjugates for urea and creatinine. *Anal. Chem.* **2010**, *82*, 9043−9049.

(11) Zheng, Z. Z.; Zhou, Y. L.; Li, X. Y.; Liu, S. Q.; Tang, Z. Y. Highly-sensitive organophosphorous pesticide biosensors based on nanostructured films of acetylcholinesterase and CdTe quantum dots. *Biosens. Bioelectron.* **2011**, *26*, 3081−3085.

(12) Dong, H. F.; Gao, W. C.; Yan, F.; Ji, H. X.; Ju, H. X. Fluorescence resonance energy transfer between quantum dots and graphene oxide for sensing. *Anal. Chem.* **2010**, *82*, 5511−5517.

(13) Gao, F.; Ye, Q.; Cui, P.; Zhang, L. Efficient fluorescence energy transfer system between CdTe-doped silica nanoparticles and gold nanoparticles for turn-on fluorescence detection of melamine. *J. Agric. Food Chem.* **2012**, *60*, 4550−4558.

(14) Zhu, X.; Chen, L.; Shen, P.; Jia, J.; Zhang, D.; Yang, L. High sensitive detection of Cry1Ab protein using a quantum dot-based fluorescence-linked immunosorbent assay. *J. Agric. Food Chem.* **2011**, *59*, 2184−2189.

(15) Liu, X.; Ni, X.; Wang, J.; Yu, X. A novel route to photoluminescent, water-soluble Mn-doped ZnS quantum dots via photopolymerization initiated by the quantum dots. *Nanotechnology* **2008**, *19*, 485602−485607.

(16) Zhang, W.; Li, Y.; Zhang, H.; Zhou, X.; Zhong, X. Facile synthesis of highly luminescent Mn-doped ZnS nanocrystals. *Inorg. Chem.* **2011**, *50*, 10432−10438.

(17) Nishino, H.; Huang, C. S.; Shea, K. J. Selective protein capture by epitope imprinting. *Angew. Chem., Int. Ed.* **2006**, *45*, 2392−2396.

(18) Tai, D. F.; Jhang, M. H.; Chen, G. Y.; Wang, S. C.; Lu, K. H.; Lee, Y. D.; Liu, H. T. Epitope-cavities generated by molecularly imprinted films measure the coincident response to anthrax protective antigen and its segments. *Anal. Chem.* **2010**, *82*, 2290−2293.

(19) KoÇ, Ì.; Baydemir, G.; Bayram, E.; Yavuz, H.; Denizli, A. Selective removal of 17β-estradiol with molecularly imprinted particle-embedded cryogel systems. *J. Hazard. Mater.* **2011**, *192*, 1819−1826.

(20) Shen, Z. H.; Huang, M. C.; Xiao, C. D.; Zhang, Y.; Zeng, X. Q.; Wang, P. G. Nonlabeled quartz crystal microbalance biosensor for bacterial detection using carbohydrate and lectin recognitions. *Anal. Chem.* **2007**, *79*, 2312−2319.

(21) Li, H. B.; Li, Y. L.; Cheng, J. Molecularly imprinted silica nanospheres embedded CdSe quantum dots for highly selective and sensitive optosensing of pyrethroids. *Chem. Mater.* **2010**, *22*, 2451−2457.

(22) Hoshino, Y.; Kodama, T.; Okahata, Y.; Shea, K. J. Peptide imprinted polymer nanoparticles: A plastic antibody. *J. Am. Chem. Soc.* **2008**, *130*, 15242−15243.

(23) Gao, D. M.; Zhang, Z. P.; Wu, M. H.; Xie, C. G.; Guan, G. J.; Wang, D. P. A surface functional monomer-directing strategy for highly dense imprinting of TNT at surface of silica nanoparticles. *J. Am. Chem. Soc.* **2007**, *129*, 7859−7866.

(24) Zhao, C. D.; Ji, Y. S.; Shao, Y. L.; Jiang, X. M.; Zhang, H. X. Novel molecularly imprinted polymer prepared by nanoattapulgite as matrix for selective solid-phase extraction of diethylstilbestrol. *J. Chromatogr., A* **2009**, *1216*, 7546−7552.

(25) Zhao, W.; Sheng, N.; Zhu, R.; Wei, F.; Cai, Z.; Zhai, M.; Du, S.; Hu, Q. Preparation of dummy template imprinted polymers at surface of silica microparticles for the selective extraction of trace bisphenol A from water samples. *J. Hazard. Mater.* **2010**, *179*, 223−229.

(26) Martin, P.; Wilson, L. D.; Jones, G. R. Optimisation of procedures for the extraction of structural analogues of propranolol with molecular imprinted polymers for sample preparation. *J. Chromatogr., A* **2000**, *889*, 143−147.

(27) Yin, Y. M.; Chen, Y. P.; Wang, X. F.; Liu, Y.; Liu, H. L.; Xie, M. X. Dummy molecularly imprinted polymers on silica particles for selective solid-phase extraction of tetrabromobisphenol A from water samples. *J. Chromatogr., A* **2012**, *1220*, 7−13.

(28) Wang, H. F.; He, Y.; Ji, T. R.; Yan, X. P. Surface molecular imprinting on Mn-doped ZnS quantum dots for room-temperature phosphorescence optosensing of pentachlorophenol in water. *Anal. Chem.* **2009**, *81*, 1615−1621.

(29) Liu, J. X.; Chen, H.; Lin, Z.; Lin, J. M. Preparation of surface imprinting polymer capped Mn-doped ZnS quantum dots and their application for chemiluminescence detection of 4-nitrophenol in tap water. *Anal. Chem.* **2010**, *82*, 7380−7386.

(30) Stringer, R. C.; Gangopadhyay, S.; Grant, S. A. Detection of nitroaromatic explosives using a fluorescent-labeled imprinted polymer. *Anal. Chem.* **2010**, *82*, 4015−4019.

(31) Lin, H. Y.; Ho, M. S.; Lee, M. H. Instant formation of molecularly imprinted poly(ethylene-co-vinylalcohol)/quantum dot composite nanoparticles and their use in one-pot urinalysis. *Biosens. Bioelectron.* **2009**, *25*, 579−586.

(32) Dirtu, A. C.; Roosens, L.; Geens, T.; Gheorghe, A.; Neels, H.; Covaci, A. Simultaneous determination of bisphenol A, triclosan, and tetrabromobisphenol A in human serum using solid-phase extraction and gas chromatography-electron capture negative-ionization mass spectrometry. *Anal. Bioanal. Chem.* **2008**, *391*, 1175−1181.

(33) Li, Y. N.; Zhou, Q. X.; Wang, Y. Y.; Xie, X. J. Fate of tetrabromobisphenol A and hexabromocyclododecane brominated flame retardants in soil and uptake by plants. *Chemosphere* **2011**, *82*, 204−209.

(34) Kitamura, S.; Suzuki, T.; Sanoh, S.; Kohta, R.; Jinno, N.; Sugihara, K.; Yoshihara, S.; Fujimoto, N.; Watanabe, H.; Ohta, S. Comparative study of the endocrine-disrupting activity of bisphenol A and 19 related compounds. *Toxicol. Sci.* **2005**, *84*, 249−259.

(35) Chu, S. G.; Haffner, G. D.; Letcher, R. J. Simultaneous determination of tetrabromobisphenol A, tetrachlorobisphenol A, bisphenol A and other halogenated analogues in sediment and sludge by high performance liquid chromatography-electrospray tandem mass spectrometry. *J. Chromatogr., A* **2005**, *1097*, 25−32.

(36) Sánchez-Brunete, C.; Miguel, E.; Tadeo, J. L. Determination of tetrabromobisphenol-A, tetrachlorobisphenol-A and bisphenol-A in

soil by ultrasonic assisted extraction and gas chromatography-mass spectrometry. *J. Chromatogr., A* **2009**, *12*, 165497−5503.
(37) Xie, Z. Y.; Ebinghaus, R.; Lohmann, R.; Heemken, O.; Caba, A.; Puttmann, W. Trace determination of the flame retardant tetrabromobisphenol A in the atmosphere by gas chromatography−mass spectrometry. *Anal. Chim. Acta* **2007**, *584*, 333−342.
(38) Zhao, R. S.; Wang, X.; Yuan, J. P. Highly sensitive determination of tetrabromobisphenol A and bisphenol A in environmental water samples by solid-phase extraction and liquid chromatography-tandem mass spectrometry. *J. Sep. Sci.* **2010**, *33*, 1652−1657.
(39) Xu, Z.; Ding, L.; Long, Y. J.; Xu, L. G.; Wang, L. B.; Xu, C. L. Preparation and evaluation of superparamagnetic surface molecularly imprinted polymer nanoparticles for selective extraction of bisphenol A in packed food. *Anal. Methods* **2011**, *3*, 1737−1744.
(40) Karim, K.; Breton, F.; Rouillon, R.; Piletska, E. V.; Guerreiro, A.; Chianella, I.; Piletsky, S. A. How to find effective functional monomers for effective molecularly imprinted polymers. *Adv. Drug Delivery Rev.* **2005**, *57*, 1795−1808.
(41) Lin, C. I.; Joseph, A. K.; Chang, C. K.; Lee, Y. D. Molecularly imprinted polymeric film on semiconductor nanoparticles analyte detection by quantum dot photoluminescence. *J. Chromatogr., A* **2004**, *1027*, 259−262.
(42) Qin, C.; Xie, M. X.; Liu, Y. Characterization of the myricetin-human serum albumin complex by spectroscopic and molecular modeling approaches. *Biomacromolecules* **2007**, *8*, 2182−2189.
(43) Zhang, W.; He, X. W.; Chen, Y.; Li, W. Y.; Zhang, Y. K. Composite of CdTe quantum dots and molecularly imprinted polymer as a sensing material for cytochrome C. *Biosens. Bioelectron.* **2011**, *26*, 2553−2558.
(44) Jiang, M.; Xie, M. X.; Zheng, D.; Liu, Y.; Li, X. Y.; Chen, X. Spectroscopic studies on the interaction of cinnamic acid and its hydroxyl derivatives with human serum albumin. *J. Mol. Struct.* **2004**, *692*, 71−80.